Oscillations of Liquid Droplets on a Horizontally Vibrating Substrate

King L. Ng[1], L. H. Carnevale[1], M. Klamka[2], P. Deuar[1], T. Bobinski[2], and P. E. Theodorakis[1]

[1]IFPAN, Institute of Physics, Polish Academy of Sciences, Warszawa, Poland

[2]Institute of Aeronautics and Applied Mechanics, Warsaw University of Technology, Warszawa, Poland

Introduction

Deformed droplets play a crucial role in industrial applications like inkjet printing, lab-on-a-chip devices, and spray cooling. Using many-body dissipative particle dynamics (MDPD), we investigate liquid droplet oscillations on a harmonically and horizontally vibrating solid substrate. Three distinct oscillation scenarios emerge: one where the droplet follows the substrate and two, more common on hydrophilic surfaces, where high shear rates lead to breakup.[1] Our simulations provide molecular-level insights into these mechanisms from an experimental perspective,[2] linking oscillation phases to contact-surface velocity and substrate wettability. The findings highlight the capillary number's role in phase behavior, offering insights for optimizing droplet dynamics in practical applications.

MDPD Model and Droplet-Substrate System

In MDPD, the equation of motion is integrated for each particle, i, which interacts with other particles, j, by means of a conservative force, F_{ij}^C, a random force, F_{ij}^R, and a dissipative force, F_{ij}^D:[3]

$$m\frac{dv_i}{dt} = \sum_{j\neq i} F_{ij}^C + F_{ij}^R + F_{ij}^D,$$

where thermal fluctuations are taken into account through random and dissipative forces in the model, and the conservative force

$$F_{ij}^C = A\omega_c(r_{ij})e_{ij} + B(\bar{\rho}_i + \bar{\rho}_j)\,\omega_d(r_{ij})e_{ij}$$

has an attractive component with $A < 0$ and a repulsive component with $B > 0$. The commonly adopted values for liquid water in MDPD have been used, where $A = -40$ and $B = 25$. We assume a smooth, unstructured, solid substrate which modeled via the Lennard-Jones (LJ) potential:

$$U^{9-3}(z') = 4\varepsilon_{\rm ws}\left[\left(\frac{\sigma_{\rm ws}}{z'}\right)^9 - \left(\frac{\sigma_{\rm ws}}{z'}\right)^3\right],$$

where $\sigma_{\rm ws} = 1$, z' is the particle-substrate distance, and $\varepsilon_{\rm ws}$ is the droplet-substrate affinity which controlls the equilibrium contact angle of the droplet.

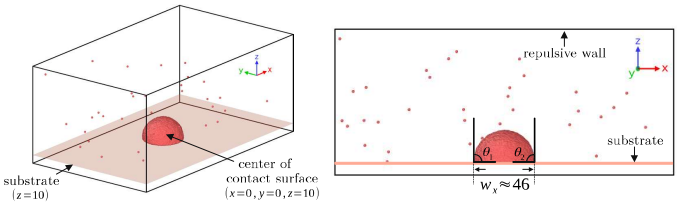

Figure 1: A typical snapshot in the simulations of a water droplet on a static substrate. In the right panel, θ_1 and θ_2 indicate the contact angles of the droplet at the two points along the contact line, as indicated. Here, the number of particles $N = 20 \times 10^4$ and the droplet–substrate affinity $\varepsilon_{\rm ws} = 2.0$, resulting in equilibrium contact angles $\theta_1, \theta_2 \approx 90°$. The droplet width at the static contact surface is $w_x \approx 46$ (MDPD unit). Snapshots were generated using OVITO software.[4]

Droplet Oscillation and Phase Diagram

In the simulation, the substrate is vibrated non-axisymmetrically (in the x direction). The vibration is controlled by the amplitude, $A_{\rm sub}$, and the frequency, $\omega_{\rm sub} = 2\pi f_{\rm sub}$, of the oscillation and remain constant throughout. The instantaneous velocity of the substrate at time t, is given by

$$u_{\rm sub}(t) = -A_{\rm sub}\omega_{\rm sub}\sin(\omega_{\rm sub}t).$$

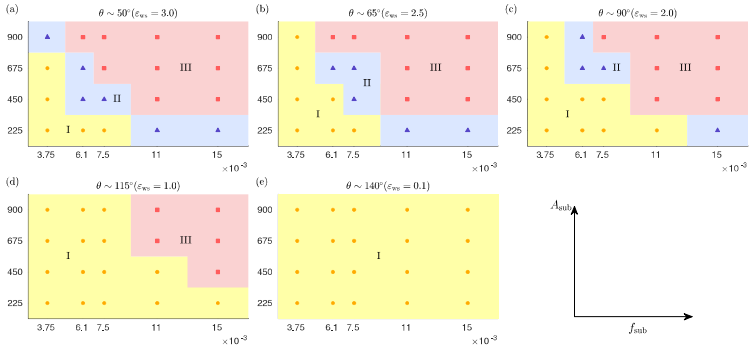

Figure 2: Phase diagram showing Phase I, II, and III as a function of the amplitude and frequency of substrate vibrations for a droplet with $N = 20 \times 10^4$ particles. Each plot corresponds to a substrate with different wettability, with the equilibrium contact angle, θ, of the droplet on a static substrate (no vibrations) indicated at the top of each plot.

Phase I Oscillation

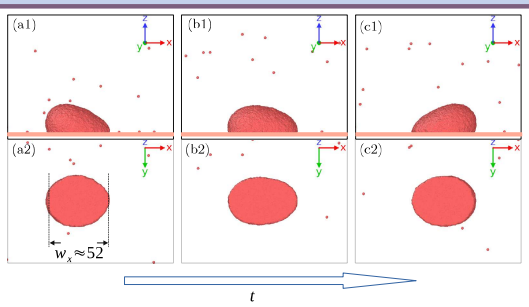

Figure 3: Example of Phase I oscillation, with time progressing from (a) to (c). $N = 20 \times 10^4$, $\varepsilon_{\rm ws} = 2.0$ ($\theta = 90°$), $A_{\rm sub} = 900$, $f_{\rm sub} = 3.75 \times 10^{-3}$. (a1) Side view; (a2) bottom view at the contact surface, taken at the same moment as (a1). (b1, b2) Side and bottom views taken one-quarter of the oscillation period after (a). (c1, c2) Side and bottom views taken one-quarter of the oscillation period after (b).

Phase II Oscillation

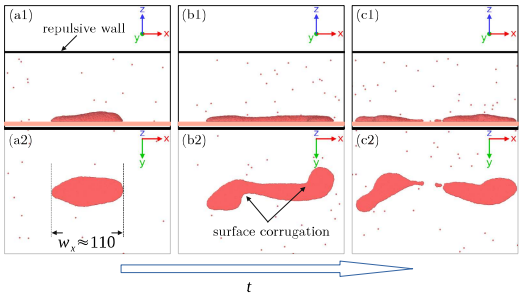

Figure 4: Example of Phase II oscillation. $N = 20 \times 10^4$, $\varepsilon_{\rm ws} = 3.0$ ($\theta = 50°$), $A_{\rm sub} = 450$, $f_{\rm sub} = 7.5 \times 10^{-3}$. The simulation box boundary is indicated. (a1) Side view; (a2) bottom view at the contact surface, at the same moment as (a1), showing the droplet in a symmetric shape. (b1, b2) Internal rotation and stretching develops, the droplet deviates significantly from a spherical-cap shape. (c1, c2) Droplet break-up occurs.

Phase III Oscillation

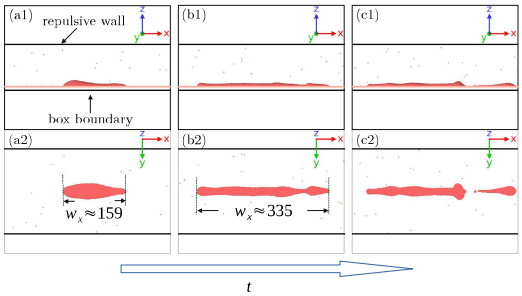

Figure 5: Example of phase III oscillation. $N = 20 \times 10^4$, $\varepsilon_{\rm ws} = 3.0$ ($\theta = 50°$), $A_{\rm sub} = 675$, $f_{\rm sub} = 7.5 \times 10^{-3}$. (a1) Side view; (a2) bottom view at the contact surface, taken at the same moment as (a1), showing the elongated configuration of the droplet. (b1, b2) Droplet is highly elongated. (c1, c2) Droplet undergoes break-up.

Phase Transition and Contact Surface Dynamics

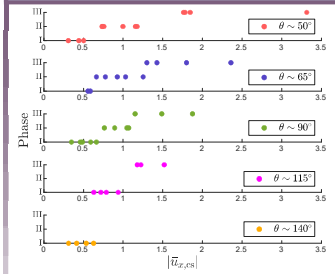

Figure 6: Phase versus the average x-velocity magnitude of the particles at the contact surface, $|\overline{u}_{x,\rm cs}|$, for droplets ($N = 20 \times 10^4$) with various equilibrium contact angles θ. Results indicate that the contact surface velocity of the droplet, and consequently the capillary number, plays a critical role in determining the three phases observed in droplet oscillation.

References

1. K. L. Ng et al., Phys. Fluids 37, 014121 (2025).
2. P. Gilewicz, M.S. thesis (Warsaw University of Technology, 2023).
3. A. P. Thompson et al., Comput. Phys. Commun. 271, 108171 (2022).
4. A. Stukowski, Modell. Simul. Mater. Sci. Eng. 18, 015012 (2010).